



DEVELOPMENT OF BODY-FITTED COORDINATE TRANSFORMATION IN FLUID  
MECHANICS REVIEW AND MODIFICATIONS

M. M. EL-REFAEE \*

ABSTRACT

This paper reviews the development of body-fitted coordinate systems for a wide variety of two-dimensional flows. The author classifies the techniques used in the body fitted transformation as: (1) algebraic techniques ( simple stretching and shearing), (2) partial differential equation techniques, and (3) conformal mapping techniques.

The conformal mapping is widely used in fluid Mechanics. It automatically stresses the regions of interest near the leading and trailing edges of airfoils. In addition, conformal mapping simplifies the kinematics aspect of the fluid mechanics problem. For these reasons, a new modified conformal mapping technique is initiated and presented in the second part of this paper. In appendix, a computer code based on this technique is listed and some few results are plotted.

1. INTRODUCTION

In the first part of the present paper, the research works of the body-fitted coordinate systems for a wide variety of two-dimensional flows were reviewed. Specifically, the following categories are considered: (i) Internal Flow (ii) External flow around a single-element airfoil (iii) flow over a multi-element airfoil system. There are, of course, other categories of flows that are important. Examples are airfoil in a wind tunnel or near ground, hydrofoil in the vicinity of a free surface etc. These additional problems can be readily tackled once the basic principles involved in the first three categories are well understood.

In each of the above three categories, there is already an extensive body of literature dealing with coordinate system generation. The author classifies the different techniques into

---

\* Assistant Professor, Aeronautical Engineering Dept.,  
King Abdulaziz University, Jeddah, Saudi Arabia

three major techniques: (1) Algebraic techniques—simple stretching, shearing etc, (2) Partial differential equation techniques where the coordinates are obtained as part of a solution of a second or fourth order partial differential equation system, and (3) Conformal mapping techniques.

In the present work, the earlier works will be briefly quoted or described according to the above classification. For each of the three categories, at least one technique for generating curvilinear coordinates will be presented in sufficient details, so that the reader may develop his own code from these details.

In the second part of this paper, a modified conformal body-fitted coordinate system around a single-element airfoil will be presented. This present approach transform the region exterior of an airfoil onto the interior of a unit circle. Fast Fourier transformation combined with the use cubic spline techniques give fast and accurate body-fitted coordinate transformation.

A computer code based on the present procedure is developed and presented in the appendix. This code will be useful in solving various fluid mechanics problems for which no analytical transformation is available.

## 2. INTERNAL FLOW PROBLEMS

Internal flow problems are of interest in such different fields as turbomachinery, bio-fluid mechanics, nuclear engineering design etc. In turbo-machinery, the flow between the blade passages is three-dimensional. This three dimensional problem is usually broken up into two two-dimensional problems[1]: (i) Flow in the blade to blade surface (ii) Flow in the hub to shroud plane. These problems may be studied as internal flow problems[2,3]. In bio-fluid mechanics, there are problems related to flow of blood through elastic, flexible blood vessels and through constructed vessels. In nuclear engineering, flow of plasma and other fluids through old-shaped vessels is an important problem. In aircraft industry the design of nacelles requires an understanding of internal flows. Thus, it is clear that an efficient grid generation technique will greatly aid in the numerical study of these and other important problems.

### 2.1 Algebraic Techniques

Two-dimensional internal flow regions can be easily treated by algebraic techniques such as simple polynomial interpolation, shearing or stretching technique. Two simple techniques, one due to Eiseman [4,5,5, &7] and the other due to McNally[8] will be chosen for detailed study here. These techniques typically take just a few seconds of CPU time to generate body-fitted coordinate systems.

#### 2.1.1 Eiseman's technique:

[We consider the region ABCD (Figure 1). Divide the curve AB as

well as CD into equal number of subregions as shown in the Fig. The length of the curve in each interval need not be the same. Let  $P_1$  be a representative point on AB, and  $P_2$  a representative point on CD.

Assume that a parameter  $t$ ,  $0 \leq t \leq 1$  varies smoothly from  $P_1$  to  $P_2$  along the specific line. Along  $P_1 P_2$ , we can assume a polynomial for  $x$  and  $y$ . For example let:  $x = at + b$ ,  $y = bt + d$ . The four unknowns  $a$ ,  $b$ ,  $c$  and  $d$  may be evaluated from  $x$  and  $y$  at  $P_1$  and  $P_2$ . At intermediate stations between  $P_1$  and  $P_2$ ,  $x$  and  $y$  may be computed by varying  $t$  in a user specified fashion.

The line from  $P_1$  to  $P_2$  is then called  $\xi$  line. Lines at intermediate points that correspond to  $t = \text{const}$  are called  $\eta$  lines. For the above case, it is clear that  $P_1 P_2$  is a straight line, since a first order polynomial is used. We can, however, use higher order polynomials also. For example, let

$$x = at^2 + bt + c, \quad y = dt + e \quad 0 \leq t \leq 1$$

The four values at the four corners give four conditions. The extra boundary condition needed is specified by setting  $(dy/dx)$  for the  $\eta$  line at any one of the end points to be such that  $\eta$  line and  $\xi$  lines are orthogonal at that point.

It is possible to increase the order of the polynomial indefinitely. However, very high order polynomials may have several inflexion points, and result in a wiggly  $\xi$  line. Eiseman[6], therefore considers the division of regions into subregions.

In figure(2) the given master region  $A_1 B_1 - G_1 H_1$  is divided into a number of subregions, with user specified lines  $C_1 D_1$ ,  $E_1 F_1$  etc. In each of the subregions a polynomial technique, is applied as shown above. By matching the slopes of the  $\xi$  line at the subregion boundaries a smooth curvilinear grid is generated. When Eiseman's technique is applied in the above manner, Eiseman calls it a multi-surface technique. Despite the simplicity of the above technique, there are certain precautions to be taken in the above technique. There is a possibility that  $\eta$  lines may intersect unless the aspect ratio of each mesh  $(\Delta\xi / \Delta\eta)$  is large. In the vicinity of concave corners,  $\eta$  lines are likely to intersect even when the aspect ratios are fairly large. Eiseman[6,7] used his coordinate generation technique, with a first order polynomial to construct a body-fitted coordinate system around a turbine blade. Turbine blades are highly curved in practice, and there is a substantial region where the turbine blade is concave (Figure 3). Eiseman estimates the line BC beyond which the  $\eta$  lines may intersect, by drawing a tangential (or osculating) circle at each point on the blade, and joining the centers of the circles. Then he restricts the grid to a line well above line BC. Since the grid is periodic it is allowed. The region in the neighbourhood of BC will describe

a grid that originates from the next, lower, blade's upper surface. Further applications of Eiseman's approach will be described in the sections on isolated and multi-element airfoils systems.

### 2.1.2 McNally's Technique:

A numerical technique for constructing nearly orthogonal coordinates was developed by Kastanis and McNally [10] as a part of their treatment of two-dimensional transonic potential flow through turbine cascades. Their procedure attempts to solve  $\nabla\xi \cdot \nabla\eta = 0$  numerically. This procedure is also a very rapid technique for constructing curvilinear coordinates like Eiseman's approach. The procedure is vulnerable near concave corners [9]. In addition, this procedure, at present is strictly applicable only for two-dimensional problems.

In axial-flow turbo-machinery, the flow is predominantly in the direction of the machine axis  $x$ . At each  $x$ -station the distance between the upper boundary and lower boundary (along  $y$  axis) is divided into equal parts (Figure 4). Joining the partitions at each  $x$  station. The streamline-like lines shown above are obtained. These are the  $\xi$  lines for the transformation. An iterative method is used to construct the  $\eta$  lines. This method is a two-iteration predictor corrector technique (Figure 5).

**Predictor:** Assume that we desire to draw an  $\eta$  lines from a point A on  $\xi_n$  to the adjacent line  $\xi_{n+1}$ . From A draw a normal to  $\xi_n$ . Let it intersect  $\xi_{n+1}$  on B. B is the "predicted" value.

**Corrector:** At B, draw a tangent to  $\xi_{n+1}$ . Draw a normal to this tangent from A. Let this normal intersect  $\xi_{n+1}$  on C.

Average positions A and B to get a new position D on  $\xi_{n+1}$ . D is the corrected value, and AD is the desired  $\eta$  line. By marching from the lower boundary towards the upper boundary step by step, the entire region may be covered by a nearly orthogonal  $\xi$ - $\eta$  curvilinear grid. The above predictor-corrector technique requires less than 10 operations per point, and requires very little CPU time. It is clear that McNally's technique requires that the spacing be very small so that the truncation errors do not accumulate as we march from one level to the next. It may also be necessary to keep the aspect ratio ( $\Delta\xi/\Delta\eta$ ) large enough to avoid intersection of  $\eta$  lines particularly in concave regions.

## 2.2 Partial Differential Equation Techniques

Partial differential equation approach includes the solution of second order (or fourth order) differential equations for the variables  $x$  and  $y$  in terms of  $\alpha$  and  $\beta$ . This technique has been applied widely by Thompson and his co-workers [10, 11 & 12] for a variety of configurations. Ghia et al [13, 14] applied a similar procedure to construct a set of body-fitted co-ordinates for a turbine cascade flow. A detailed discussion of this

method, its merits and drawbacks are postponed until the next section, where we deal with coordinate systems for isolated airfoils.

### 2.3 Conformal Mapping Techniques

Body fitted coordinate systems have been constructed by several workers using conformal mapping techniques to transform the internal flow region into a rectangular polygon. Thom and Apelt[15] used  $\phi - \psi$  lines as  $\eta - \xi$  coordinates. Barfield[16] used the complex Green's function to map an irregular flow region into the unit circle, and then to the edges of a rectangular polygon through Schwarz christoffel transformation. The interior points were determined by point successive over-relaxation of the inverse laplace equations. In the work of Thom and Apelt, the  $\phi$  and  $\psi$  lines were determined as follows. Laplace equation was first solved iteratively to determine the value of one coordinate  $x$  both in the interior and along the boundaries of the transformed region. The conjugate coordinate variable  $y$  was then constructed by integration using Cauchy-Riemann condition. With square mesh in the transformed plane, they found that for some geometries, it was not always possible to obtain a mesh properly fitted to the physical region with their approach. Hung and Brown[17] obtained an exact fit between the physical region and the transformed region using a dual iterative procedure which was an extension of Thom and Apelt's basic approach. In order to obtain an understanding of how conformal mapping techniques may be used to map interval flow regions onto rectangles, we briefly describe the procedure due to Hung and Brown here. Region ABCD is the flow region that is mapped onto  $A_1 B_1 C_1 D_1$  in the conformal  $\xi - \eta$  plane (Figure 6). For convenience, at downstream boundary, the  $\xi$  grid is assumed parallel to the  $x$  axis. The iterative procedure for conformal mapping involves the following steps: (i) At AD,  $x = x_1$ . At BC,  $x = x_2$ . On AB assume an  $x$  distribution. Laplace equation is applied in the region  $A_1 B_1 C_1 D_1$  including nodes on  $D_1 C_1$  where one-sided differences are used to approximate  $x_{\eta\eta}$ . The values of  $x$  on AB are updated using the values at the adjoining nodes and symmetry conditions. Laplace equation is solved again. This procedure is repeated a number of times till  $x$  values converge every where; (ii) values of  $y$  on the wall are obtained from the geometry of the wall. New inlet and outlet values of  $y$  along  $A_1 D_1$  and  $B_1 C_1$  are determined from the fact that  $x$  and  $y$  are conjugate functions in the regions considered i.e,

$$\text{and } -y_{\xi} = x_{\eta} \quad \text{and} \quad X_{\xi} = y_{\eta}$$

$$y_{1,j+1} = y_{1,j} + \int_j^{j+1} \left( \frac{\partial x}{\partial \xi} \right) d\eta$$

Hung and Brown used fourth-order accurate numerical integration formulas to evaluate  $y$  along  $A_1 D_1$  and  $B_1 C_1$ . Because of accu-

To minimize numerical errors, the integrated values of  $y$  for the wall at the inlet and outlet may not coincide with those obtained from the wall geometry. In such a case the difference is distributed proportionately over the inlet and outlet sections with these adjusted values of  $y$  on the boundary, at the interior nodes,  $y$  is determined by solving

$$y_{\xi\xi} + y_{\eta\eta} = 0 \quad \text{in the region } A_1 B_1 C_1 D_1$$

(iii) the  $x$  field is now determined from the formula

$$x_{i+1,j} - x_{i,j} = - \int_{i,j}^{i+1,j} \left( \frac{\partial y}{\partial \eta} \right) d\xi$$

for all nodes in the flow field including those on the boundary. The  $x$  field thus obtained will not be compatible with the  $x$  field obtained from step (i). In fact  $x_{IMAX,j}$  may be less than  $x_2$  for all  $1 \leq j \leq JMAX$  or  $x_{IMAX,j}$  may exceed  $x_2$  for all  $1 \leq j \leq JMAX$ . In such a case adjust  $IMAX$ , so that  $IMAX_{new} = IMAX \pm 1$ ; (iv) With the newly defined  $IMAX$ , and the boundary values for  $x$ , steps (i) through (iii) are repeated until the distribution of  $y$  on either end has converged; (v) When the  $x, y$  fields have converged, the main iteration loop (i-iv) is exited. At  $I = IMAX$  and  $1 \leq j \leq Jmax$ , we have in general:

$$x_{IMAX-1,j} < x_2 < x_{IMAX+1,j} \quad \text{and}$$

$\xi_{MAX} = (IMAX-1)\Delta\xi$  at  $IMAX$ . We determine an average  $\bar{\alpha}_{IMAX}$  so that, on an average, at  $\alpha = \bar{\alpha}_{IMAX}$ ,  $x = x_2$  for all  $j$ .

$$\text{i.e. Let } \alpha_{Imax,j}^{new} = \alpha_{Imax-1,j}^{old} + \frac{\Delta\alpha}{[\alpha_{IMAX-1,j}^{x_2} - \alpha_{IMAX,j}^{x_2}]}$$

$$\text{Then } \bar{\alpha}_{IMAX}^x = \frac{1}{JMAX} \sum_{j=1}^{JMAX} \alpha_{IMAX,j}$$

$$\text{Also } \Delta\alpha_{New} = \bar{\alpha}_{IMAX} / (IMAX-1)$$

with  $\Delta\alpha_{new}$  and  $\Delta\alpha$ , and with the boundary condition  $x = x_1$  at  $\eta = 1$  and  $x = x_2$  at  $I = IMAX$ , the Laplace equation for  $x$  is solved to get a final solution for  $x$ .

It is clear that the above procedure of Hung and Brown although very accurate, may prove to be time consuming since it involves repeated solution of Laplace equation in a rectangular grid. A new approach for conformal coordinates generation discussed in the last section of this report may be considerably faster than the procedure outlined above, particularly when no starting (guess) solution is available for  $x$  and  $y$ . Conformal mapping techniques have been used by other workers to study internal flows. Ives [18] develops a solution proce-

ture for studying transonic cascade flow. Jameson[19] and Chen[20] studied a conformal mapping technique for the transonic macelle problem (axi-symmetric). Caughey[21] extended the conformal mapping to include a central body as well. In these cases a simple shearing transformation has applied together with a series of conformal transformations. The shearing transformation made the transformed coordinates slightly non-orthogonal, but greatly simplified the subsequent analysis.

### 3. FLOW AROUND SINGLE-ELEMENT AIRFOILS

As in the case of internal flow problems, the various techniques for generation of body-fitted coordinate system around isolated airfoils may be broadly classified as (i) Algebraic techniques, (ii) Elleptic differential equation techniques and (iii) conformal mapping techniques.

#### 3.1 Algebraic Techniques:

As the name implies, this approach makes use of simple, algebraic stretching and shearing relationships to construct the curvilinear coordinate grid. The CPU time required to construct a grid using algebraic relationships is very negligible therefore, in problems involving repeated computation of the curvilinear network e.g. free surface flow[22] aileron Buzz[23] etc. Algebraic techniques are the most practical ones. Some of the common methods that utilize algebraic relationships are described here.

##### (i) Shearing transformation

The simple shearing transformation is given by:

$\xi = x$  ,  $\eta = y - y_s(x)$  where  $y_s$  is the equation that describes the surface.

Shearing transformations are not usually advised for thick airfoils and blunt nosed airfoils because of the abrupt change in the slope of the  $\xi$  lines. For thin airfoils shearing airfoil provides a rapid method for generation of body fitted grid. Shearing transformations have been used also for compression corner problems by Carter[24], Hung and McCormark[25], Hankey and others.

##### (ii) Eiseman's multi-surface technique:

Eiseman's multi-surface technique was introduced in the previous section on internal flows. The grid system for the shock-blunt body problem may be thought of as an outcome of Eiseman's scheme when the interpolation functions are chosen to be linear. For the single-element airfoil system, two types of grids-the O grid and the C grid-are possible (Figure 7). In his work on aileron buzz, Steger[23] discusses the relative merits of the two grids. For viscous flow problems that use vorticity as a dependent variable, the O type of grid wastes a lot of nodes in

the non-vortical region while the C type of grid efficiently packs the nodes in the vortical region. Of course, in order to specify the far field boundary condition reasonably accurately, the boundary of C grid must still be far away from the body unless some explicit relationships, such as the integral relationship used by Wu[26] and his co-workers, is used to specify the far field boundary condition accurately. If such an integral relationship is used, the outer boundary of the C type of grid may be placed just outside the edge of the vortical region.

Eiseman's approach may be used on both kind of grids between a point  $P_1$  and  $P_2$ , both  $x$  and  $y$  are taken as polynomials in  $t$ , where  $t$  varies smoothly from 0 to 1. By imposing edge condition at  $P_1$  and  $P_2$ , and slope conditions if necessary, the shape of the line  $P_1 P_2$  is uniquely defined. The  $\xi$  lines are obtained by joining all the points that have a constant  $t$ . If necessary, user may specify additional intermediate surfaces.

As in the two-dimensional internal flow case, Eiseman's approach can cause difficulties if the mesh aspect ratio is not large enough or if the body is concave in some regions.

### 3.2 Elliptic Differential Equation Techniques

The idea of generating curvilinear coordinate systems as a result of solving elliptic partial differential equations was first proposed by Winslow [27], Chu [28] and other workers. In recent years, this idea has been developed into a powerful technique for body-fitted coordinates generation by Thompson, [10,12] and others [29]. This technique is powerful because it can be applied with minor modifications to internal flows, single and multiple element airfoil systems, and even to three dimensional flows [23]. This technique is discussed here in some detail. The merits as well as the drawbacks of this technique are presented.

In principle, the numerical transformation procedure consists of determining the boundary-oriented coordinates  $\xi$  and  $\eta$  as the solution of the following equations

$$\begin{aligned} \xi_{xx} + \xi_{\phi\phi} &= Q & \phi &= y \text{ for 2-D case} \\ & & &= r\theta \text{ for axi-symmetric cases} \\ \eta_{xx} + \eta_{\phi\phi} &= R \end{aligned}$$

The functions  $Q$  and  $R$  are called forcing function and they are introduced in order to concentrate or spread out coordinate lines at desired locations. In the  $\xi$ - $\eta$  plane it may be shown that the above equations take on the following form:

$$\begin{aligned} a\phi_{\eta\eta} + 2b\phi_{\xi\eta} + e\phi_{\xi\xi} + J^2 (Q\phi_{\eta} + R\phi_{\xi}) &= 0 \\ a x_{\eta\eta} + 2bx_{\xi\eta} + cx_{\xi\xi} + J^2 (Qx_{\eta} + Rx_{\xi}) &= 0 \end{aligned}$$

where  $a = \phi_{\xi}^2 + x_{\xi}^2$  ;  $b = -(\phi_{\xi}\phi_{\eta} + x_{\xi}x_{\eta})$

$$c = \phi_{\eta}^2 + x_{\eta}^2 \text{ and } J = \phi_{\eta} x_{\xi} - \phi_{\xi} x_{\eta}$$

The above equations are non-linear, but elliptic. Therefore it should be possible to apply relaxation procedures, such as those used in subsonic potential flow problems, to solve these equations. The forcing functions R and Q are chosen to be of the following form:

$$R = - \sum_{m=1}^{MMAX} a_m \frac{\xi - \xi_m}{|\xi - \xi_m|} \exp [ - c_m |\xi - \xi_m| ]$$

$$- \sum_{n=1}^{NMAX} b_n \frac{\xi - \xi_n}{|\xi - \xi_n|} \exp [ - d_n \sqrt{(\xi - \xi_n)^2 + (\eta - \eta_n)^2} ]$$

$$Q = - \sum_{m=1}^{MMAX} a_m \frac{\eta - \eta_m}{|\eta - \eta_m|} \exp [ - c_m |\eta - \eta_m| ]$$

$$- \sum_{n=1}^{NMAX} b_n \frac{\eta - \eta_n}{|\eta - \eta_n|} \exp [ - d_n \sqrt{(\xi - \xi_n)^2 + (\eta - \eta_n)^2} ]$$

$a_m$ ,  $b_n$ ,  $c_m$  and  $d_n$  are arbitrary coefficients. P and Q usually increase in magnitude with the concentration of the grid. For high Reynolds number flows, P and Q will be very high.

The second order and fourth order elliptic equations are the popular candidates because they obey what is known as a maximum or minimum principle. If Laplace equation for  $\xi$ , for example, is solved subject to some specified boundary conditions, the maximum principle ensures that  $\xi$  will attain its maximum value only on the boundaries of the region and not in the interior. Thus maximum principle prevents cross-over of like-coordinate lines everywhere, even when concave regions and similar critical regions are present.

Both O type of grid and C type of grid may be generated by the partial differential equation technique. At the cuts, periodic conditions may be employed (Figure 8). The advantages of the partial differential equation approach are:

- (1) Its simple logic. The theory behind this approach is not overly complex. It is easy to code the above approach, and apply the procedure to a variety of internal and external flow problems.
- (2) Its provision for grid control. If R and Q are not excessively large, they provide the desired control over grid spacing in critical regions.
- (3) Availability of a wide body of literature and computer codes that apply this approach to a variety of problems

The disadvantages are:

- (1) The resulting grid is non-orthogonal, and in some cases highlywarped.

(2) Very slow convergence. Particularly at high Reynolds numbers. As the magnitudes of  $Q$  and  $R$  increase, the partial differential equations become very stiff and converge very slowly. In some cases the final solution contains a number of wiggles. It may be shown that these wiggly solutions are the correct solutions for the difference equations.

(3) Boundary conditions: If  $P$  and  $Q$  are very large, the Dirichlet boundary conditions on the solid must, in a sense be consistent with the forcing function. Some authors try to get around the specification of consistent Dirichlet conditions, by specifying Neumanon type of boundary conditions. But in some cases the Neumann condition, together with large  $P$  and  $Q$ , violates the maximum principle at least numerically and permits cross over of  $\xi$  lines or  $\eta$  lines.

### 3.3 Conformal Mapping Techniques

Conformal mapping of an arbitrary airfoil onto a unit circle or to the lower part of half plane has been a topic of great interest to research workers for several years. Historically, Theoderson [30] studied the numerical transformation of single and multi-element airfoil. The well-known Karman-Trefftz transformation maps a biconvex airfoil onto a unit circle [31]. In 1966, Skulsky [32] presented a numerical mapping procedure for arbitrary airplane cross sections and applied this technique to study the cross flow past a slender body.

In recent years, transonic flow calculations have given a new momentum to be search for a rapid, accurate conformal mapping procedure. The viscous displacement effects are important in transonic flows. Many transonic potential flow codes [33,34] include viscous displacement effects to improve the reliability of the numerical solution. The displacement thickness is calculated every few iterations using a simple integral procedure such as the Nash-McDonald procedure, [35] and a new body shape is calculated. Thus every few iterations, it is necessary to conformally map a new body onto a circle. This calls for highly efficient, rapid numerical techniques.

Jameson [36] used a sheared parabolic coordinate system to study flow over airfoils and wings. His transformation is a very rapid mapping procedure. While Jameson's procedure is rapid and well-suited for three dimensional flow problems, for two-dimensional problems, a slower but accurate numerical conformal mapping onto a unit circle is preferred. Both Ives [37], Bauer et al [38] and Eriksson [39] have developed procedures for mapping airfoils onto unit circles. The code generated by Bauer et al has the additional feature of treating airfoils open at the trailing edge.

## 4. MULTI-ELEMENT AIRFOIL COORDINATE SYSTEM

### 4.1 Algebraic Techniques

Simple shearing techniques and algebraic techniques tend to become increasingly complex for multi-element coordinate sys-

tems. Eiseman applied his multi-surface method to generate a curvilinear coordinate system. The blending of coordinates around the two airfoils was accomplished through an intermediate cartesian coordinate system. It is clear that such algebraic techniques can be used to generate curvilinear coordinates only through a considerably amount of trial and error. Thus the low CPU requirements of algebraic techniques are more than offset by the increased amount of man-hours spent in algebraic approaches.

#### 4.2 Partial Differential Equations Approach

The code TOMCAT[10,11] developed by Thompson is capable of analysing a number of airfoils in the flow field. Through the introduction of cuts in the computational field, and the specification of appropriate periodic or coordinate continuity conditions, the grid generation equations may be solved on a rectangular transform. For a typical two-body airfoil problems the boundaries in the physical and transformed planes are shown in Figure (9). In solid boundaries BC, DD<sub>1</sub>, and CC<sub>1</sub>, Dirichlet boundary conditions are usually specified. At the branch cut DC, AB periodic conditions are imposed.

#### 4.3 Conformal Mapping Techniques

Theoderson[30] was one of the first workers to study conformal representation of multiple element airfoils. Ives work on conformal mapping of single element airfoils[37] also contains extensions to two-and multi-element airfoil systems. In Ives approach for two-element airfoils the point at infinity is mapped into a singular point inside the computational region. Caution may be required when differencing the flow variables in the neighbourhood of this singular point. Ives also has developed a conformal mapping procedure for a cascade of airfoils.

### 5. MODIFIED BODY-FITTED COORDINATE SYSTEM (FOR A SINGLE ELEMENT AIRFOIL)

Let us consider the transformation of the region exterior of an airfoil onto the interior of a unit circle. Let  $z = x+iy$  and  $\sigma = \frac{1}{\sigma} e^{-i\theta}$  be the corresponding points exterior to the profile and the unit circle. Let  $H = \left| \frac{dz}{d\sigma} \right|$  be the desired transformation factor. If  $\epsilon$  is the included angle at the trailing edge, using a series of N terms one can set,

$$\frac{dz}{d\sigma} = \left(1 - \frac{1}{\sigma}\right)^{1 - \frac{\epsilon}{\pi}} \exp \left[ \sum_{n=0}^N \frac{c_n}{\sigma^n} \right]$$

This method of representing the transformation has the advantage that it allows a profile with an open tail to be mapped to a closed circle. Expanding the above series, it may be shown that the coefficient of the term  $1/\sigma$  is

$$\bar{c} = \left[ c_1 - 1 + \frac{6}{\pi} \right] \exp(c_0)$$

Then, according to the Cagely integral theorem; integration of  $dz/d\sigma$  around any closed curve exterior to the unit circle in the  $\sigma$  plane results in a fixed gap

$$Z_2 - Z_1 = 2\pi i \bar{c}$$

This gap can be used to set a desired wake gap.

The mapping coefficients may be calculated using a simple iterative procedure (Figure 10). Let  $\beta$  and  $s$  be the tangent angle and the arc length of the profile. Let

$$C_n = a_n - ib_n$$

$\beta$  is available as a function of  $s$ .

Taking the Logarithm of the series for  $dz/d\sigma$ , and separating it into real and imaginary parts, for  $r = 1$ , one obtains,

$$\log \frac{ds}{d\theta} = +\left(1 - \frac{\epsilon}{\pi}\right) \log \left(2 \sin \frac{\theta}{2}\right) + \sum_{n=0}^N a_n \cos n\theta + b_n \sin n\theta \quad (A)$$

$$\beta + \theta + \frac{\pi}{2} - \left(1 - \frac{\epsilon}{\pi}\right) \frac{\theta - \pi}{2} = \sum_{n=0}^N a_n \sin n\theta - b_n \cos n\theta \quad (B)$$

Given an estimate for  $s(\theta)$ , the arc length of the airfoil profile as a function of the angle  $\theta$  in the circle plane, we can calculate the coefficients  $a_n$  and  $b_n$  from equation B. Since  $a_n$  and  $b_n$  are known, the conjugate Fourier series in equation A may be constructed, and  $\log(ds/d\theta)$  evaluated. The resulting value of  $(ds/d\theta)$  may be integrated to give a new estimate of  $s(\theta)$ .

The iterations converge quite rapidly. It is convenient to use a series with  $K$  terms to represent the mapping function at  $2K$  equally spaced mesh points around the circle. The use of fast Fourier transform allows the number of operations in the evaluation of Fourier series to be  $O(K \log K)$ , whereas conventional techniques would require  $O(K^2)$  operations. The use of cubic spline techniques to curve fit and interpolate  $s(\theta)$ ,  $\beta(s)$  etc. is also desirable.

A computer code based on the above procedure is included at the end of the appendix. A number of flow calculations performed by the workers at Georgia Tech. have demonstrated the advantages of a conformal mapping systems for incompressible and compressible calculations[26]. It is hoped that this code will aid the workers in treating problems for which no analytical transformation is available.

#### APPENDIX

In the following pages, a computer program for numerically performing the conformal transformation of any airfoil (both open and closed trailing edge) onto a circle is described. The theory behind the conformal transformation was already described

in the section 5.

The present program contains many subroutines such as a successive over-relaxation subroutine for computing x and y coordinates in the interior of the computational domain, several cal-comp plotter instructions to display the  $\eta - \xi$  lines in the physical domain, and a subroutine for numerically computing the apparent mass properties of the airfoil. The following subroutines are used in the above computer program.

**MAIN:** The main program controls the flow of information between subroutines. The data is also read in the main program. The final grid is also written on TAPE3, through FORTRAN statements in the main program. The main program also executes the iterative procedure, and plots the final output.

**Subroutine MAP:** The MAP subroutine computes  $H = |dz/d\sigma|$  on a  $120 \times 30$  grid analytically, by evaluating the series for  $(dz/d\xi)$ . The MAP subroutine also calls the subroutine APMASS.

In viscous flow calculations, one may compute H either through MAP subroutine or numerically from the final (x-y) grid. Since the final (x-y) grid is tailored to user's needs, and because numerical evaluation of H from x and y involves very few arithmetic operations, the numerical evaluation of H is recommended.

**Subroutine APMASS:** Subroutine APMASS computes the apparent mass properties of the airfoil, following the numerical conformal transformation. The six coefficients  $m_{xx}$ ,  $m_{xy}$ ,  $m_{xw}$ ,  $m_{yw}$  and  $m_{ww}$  are evaluated through a numerical integration in the  $\xi$  plane.

**Subroutine RELAX:** This subroutine computes the (x-y) grid in the circular plane through a point by point successive over relaxation technique, with a relaxation factor of 1.8.

The subroutine RELAX: Solves the equation

$$\frac{\partial^2 \phi}{\partial r^2} + \frac{1}{r} \frac{\partial \phi}{\partial r} + \frac{1}{r^2} \frac{\partial^2 \phi}{\partial \theta^2} = 0 \quad \text{subject to Dirichlet boundary conditions, } \phi \text{ may be } x \text{ or } y. \quad \text{In this subroutine, I assure}$$

$$r = \frac{1}{1-\eta} \quad \eta = \frac{j-1}{j_{\max}}$$

Thus r varies from 1 to  $\infty$  as  $\eta$  varies from 0 to 1.

After applying central differences, one obtains

$$A\phi_{i,j} + B\phi_{i+1,j} + C\phi_{i,j+1} + D\phi_{i-1,j} + E\phi_{i,j} = 0$$

The user may specify his own variations of r as a function of  $\eta$ . In this case, one only needs to replace the A, B, C, and E coefficients in the RELAX subroutine by working out the finite difference expression.

**Subroutine CONJ:** Evaluates the conjugate component of an analytical function  $(\phi + i\psi)$ , i.e. given  $\phi$  on a unit circle  $\psi$  is

evaluated, and vice versa.

Subroutine FFORM: This subroutine performs the fast Fourier transform operations to determine the Fourier coefficients of a complex function.

Subroutine FOUCF: Determines the Fourier coefficients of a complex function. Though the bulk of the arithmetic work is performed in subroutine FFORM, the subroutine FOUCF feeds the input to FFORM, and also unscrambles the output from FFORM.

Subroutine SPLIF: Given  $F(s)$  where  $s$  is a monotonically increasing independent variable, SPLIF constructs a cubic spline fit, satisfying specified end conditions.

Subroutine INTPL: Given  $F(s)$  as a function of  $s$  (and the derivatives  $F'(s)$ ,  $F''(s)$  and  $F'''(s)$  usually obtained from a call to SPLIF), the subroutine INTPL interpolates to find  $F(s_1)$  at any user specified  $s_1$  value.

#### Program Input:

Card 1: Title : FORMAT (1x, 16A4, I4)

Card 2: FUN, FNL, EPSIL, FORMAT (5F 10.7)

FNU: Total no of points on the upper surface including nose and tail

FNL: Total no. of points on the lower surface including nose and tail.

EPSIL: Trailing edge angle divided by if known. Otherwise set to zero.

Card 3: Coordinates at the nose x,y FORMAT (2F 10.7)

Card 4: Coordinates of points on upper surface

Card 5: "

Card 6: "

Card FNO + 2 Coordinates at trailing edge

Card FNO + 3 Coordinates at nose

Card FNU + 4 "

Card FNU + FNL + 2 Coordinates at trailing edge

Card FNU + FNL + 3 IMAX , JMAX, DELTA FORMAT (2I

where: Imax, Jmax are grid dimensions set to zero and DELTA set to zero in  $r-\theta$  plane.

#### Output

The output from the program falls into three categories:

1- Paper output: The paper output consists of the following:

- (1) The input data is printed out to check and correct errors in input data
- (2) The convergence history of the iterative procedure is printed out. After convergence, the coefficients of the Fourier series in the analytical expression for  $|dz/d\sigma|$  are also printed out

(3) The apparent mass properties of the airfoil are printed out. In addition, the coefficients  $\xi, \eta$ , in the series

$$Z = \xi + \eta i + \dots$$

are printed out.

(4) IMAX, JMAX - the dimensions of the grid that is finally obtained in the program. IMAX and JMAX are also printed out.

## 2- Plotter Output

The computational grid is plotted using calcomp subroutines to obtain a visual display of the final grid.

## 3- Disk output

The final grid (x,y) is written on TAPE3 for later use according to the following FORMAT:

```
WRITE (3, 590) ((X(I,J), J = 1, JMAX), I = 1, IMAX)
```

```
WRITE (3, 590) ((Y(I,J), J=1, JMAX), I = 1, IMAX)
```

```
590 FORMAT (10 F12.8)
```

### Suggestions and Modifications:

Some of the suggestions and modifications are already pointed out on the program listing. In addition, the following modifications are desirable.

(i) If x and y are calculated a number of times; replace the slow RELAX subroutine with some faster poisson solver.

(ii) The final output is on a (60x30) or (40x30) or (30x30) grid. In some cases, the user may desire a grid (48x40) for example. In such a case,

(a) Run the program as it is, on a (60x30) grid

(b) Post-process the solution on TAPE 3.

Using SPLIF and INTPL subroutines, the solution on TAPE3 can be interpolated to get data on any grid with no determination of data.

## REFERENCES

1. Erdos, J., Alzner, E., Kalben, P., McNally, W. and Slutsky, S., "Time-Dependent Transonic Flow Solutions for Axial Turbomachinery", Aerodynamic Analysis Requiring Advanced Computers, Vol. 1, pp. 587-621, NASA sp-347, 1975.
2. Knight, D. D., "Application of Curvilinear Coordinate Generation Techniques to the Computation of Internal Flows," Numerical Grid Generation, edited by J. F. Thompson, North-Holland, 1982.
3. Deese, J. E. and Agarwal, R. K., "Calculation of Axisymmetric Inlet Flow Field Using the Euler Equations," AIAA Paper 83-1853, Danvers, Mass. 1983.

4. Eiseman, P. R., "A Multi-Surface Method of Coordinate Generation", Journal of Computational Physics, # 24, 1978.
5. Eiseman, P. R., "Coordinate Generation With Precise Controls Over Mesh Properties," Journal of Computational Physics, Vol. 47, 1982, p. 331.
6. Eiseman, P. R., "Adaptive Grid-Generation by Mean Value Relaxation," Advances in Grid Generation, ASME Fluids Engineering Conference, Houston, June 1983.
7. Eiseman, P. R., "Alternating Direction Adaptive Grid Generation," AIAA Paper 83-1937, Danvers, Mass. 1983.
8. Katsanis, T. and McNally, W. D., "FORTRAN Program for Calculating Velocities and Streamlines on the Hub-shroud Mid-Channel Flow Surface of an Axial-or Mixed-Flow Turbomachine. I-User's Manual NASA TN D-7343, 1973.
9. Vinokbly, M. and Lombard, G. K., "Algebraic Grid Generation with Corner Singularities," Advances in Grid Generation, ASME Fluids Engineering Conference, Houston, June, 1983.
10. Thompson, J. F., Warsi, Z. U., and Mastin, C. W. Boundary-Fitted Coordinate Systems for Numerical Solution of Partial Differential Equations," Journal of Computational Physics, Vol. 47, 1982.
11. Thompson, J. F., and Mastin, C. W., "Order of Difference Expressions In Curvilinear Coordinate Systems," Journal of Fluids Engineering, Vol. 107, June, 1985.
12. Thompson, J. F., "Grid Generation Techniques in Computational Fluid Dynamics," AIAA Journal, Vol. 22, No. 11, November, 1984.
13. Ghia, U. and Ghia, K. N., "Numerical Generation of a System of Curvilinear Coordinates for Turbine Cascade Flow Analysis", University of Cincinnati Report No. AFL-75-4-17, 1975.
14. Ghia, K. N., Ghia, U., and Shin, C. T., "Adaptive Grid Generation for Flows with Local High Gradient Regions," Advances in Grid Generation ASME Fluids Engineering Conference, Houston, June, 1983.
15. Thom, A. and Apelt, C. J., "Field Computations in Engineering and Physics," Van Nostrand, London, 1961.
16. Barfield, W. D., "Numerical Method for Generating Orthogonal Curvilinear Meshes," Journal of Computational Physics, Vol. 11, March, 1973, pp. 348-359.
17. Hung, T. K. and Brown, T. D., "An Implicit Finite-Difference Method for Solving the Navier-Stokes equation using Orthogonal Curvilinear Coordinates", Journal of Computational Physics, 1977, pp. 343-36 .
18. Ives, D. C. and Livtermoza, J. F., "Analysis of Cascade Flow Using, Conformal Mapping and Relaxation Techniques", AIAA Paper No. 76-370, Ninth Fluid and Plasma Dynamics Conf. 1976.

19. Caughey, D. A., and Jameson, A., "Accelerated Iterative Calculation of Transonic Nacelle Flow Fields", AIAA Paper 76-100, 1976.
20. Chen, L. T., "A Nearly Conformal Grid-Generation Method for Transonic Wing-Body Flow Field Calculations," AIAA Paper 82-0108, Orlando, Fla, Jan. 1982.
21. Caughey, D. A., "A Systematic Procedure for Generating Useful Conformal Mappings", International Journal for Numerical Methods in Engineering, Dec. 1978.
22. Wetch, J. E., Harlow, F. H., Shannon, J. P., and Daly, B. J., "The MAC Method: A Computing Technique for Solving Viscous Incompressible, Transient Fluid-Flow Problems Involving Free Surfaces", Los Alamos Scientific Laboratory Report LA-3425.
23. Steger, J. L., "Calculation of Transonic Aileron Buzz," AIAA Paper 79-0134, 1979.
24. Carter, J. E., "Numerical Solutions of the Supersonic Laminar Flow Over a Two-Dimensional Compression Corner", Lecture Notes in Physics, Vol.19, S. Verlag, 1973.
25. Hung, C. M. and MacCormack, R. W. "Numerical Solution Supersonic Laminar Flow Over a Three-dimensional Compression Corner", AIAA Paper 77-694, June 1977.
26. Wu, J. C. and El-Refaee, M., "Solutions of the Compressible Navier-Stokes Equations Using the Integral Method," AIAA Journal, Vol. 20, (1982).
27. Winslow, A. J., "Numerical Solution of the Quasi-Linear Poisson Equation in a Non-uniform Triangular Mesh," Journal of Computational Physics, 2, 149 (1966).
28. Chu, W. H., "Development of a General Finite Difference Approximation for a General Domain", Journal of Computation Physics, Vol. 8, Dec. 1971, pp. 392-408.
29. Christov, C. I., "Orthogonal Coordinate Meshes with Manageable Jacobian, "Numerical Grid Generation, edited by J. F. Thompson, North-Holland, 1982.
30. Theoderson, T. and Growick, I.E., "General Theory of Arbitrary Wing Sections," NACA TR No. 452, 1933. Also Gavick, I.E., "Potential Flow about Arbitrary Biplane Wing Sections", Rept. 542, NACA, 1936.
31. Von Karman, T. and Trepptz, E., Zeitschrift-fur Flug techniche... vol. 9, 1918, pp. 111-116.
32. Sbulsky, R. S., "A Conformal Mapping Method to Predict Low-speed Aerodynamic Characteristics of Arbitrary Slender Re-Entry Shapes", Journal of Spacecraft and Rockets, Vol. 3, No. 2, Feb. 1966, pp. 247-253.
33. Bauer, F., Garabedian, P., Korn, D. and Jameson, A., "Supercritical Wing Sections II", Springer-Verlag, New York, 1975,

34. Shankar, U, and Rudy, S., "Application of a Two-Dimensional Grid Solver for Three-Dimensional Problems," AIAA Journal, Vol. 23; No. 3., 1984.
35. Nash, J. F. and Macdonald, A. G. J., "The Calculation of Momentum Thickness in a Turbulent Boundary Layer at Machalumbers upto Unity", Aeronautical Research Council C. P. No. 963, London, 1967.
36. Jameson, A. and Caughey, D. A., "Numerical Calculation of the Transonic Flow Past a Swept Wing", NASA-CR-153297, June 1977. (Available from Georgia Tech. Library in Microfiche from : N77-27071).
37. Ives, D. C., "A Modern Look at Conformal Mapping Including Multiply Connected Regions", AIAA Journal, Vol. 14, No. 8, 1976, pp. 1006-1011.
38. Bauer, F., Garabedian, P. and Korn, D. "Supercritical Wing Sections III", Springer-Verlag, New York, 1977. (Library Call No. TL570. B365).
39. Eriksson, L. E., "Generation of Boundary-Conforming Grids Around Wing-Body Configurations Using Transfinite Interpolation", AIAA Journal, Vol. 20, No. 10, Oct. 1982.

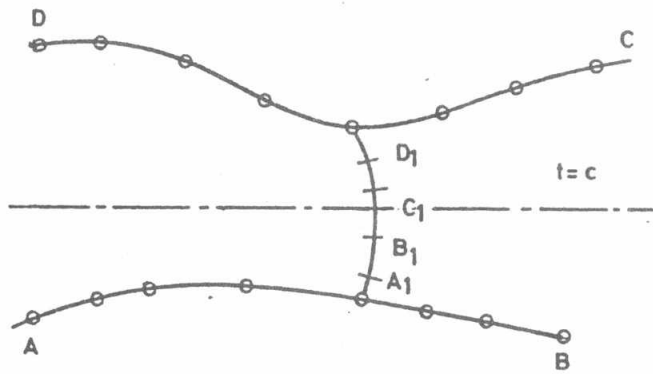


Fig. 1.

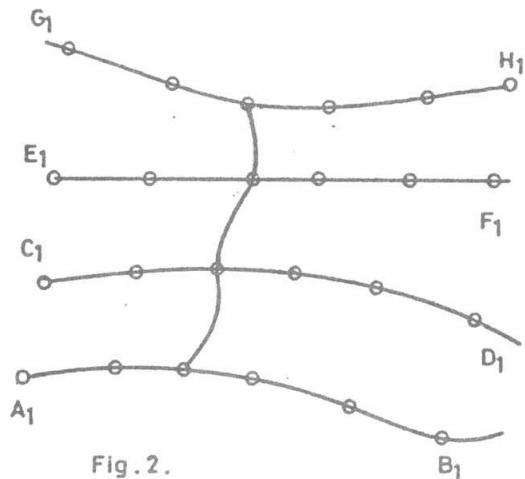


Fig. 2.

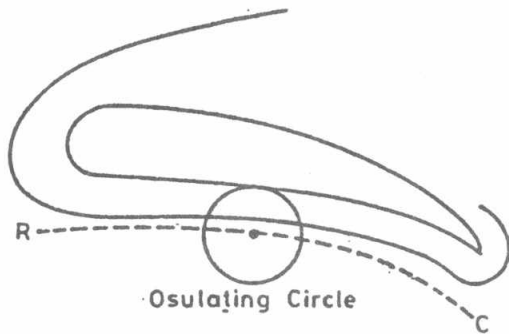


Fig. 3.

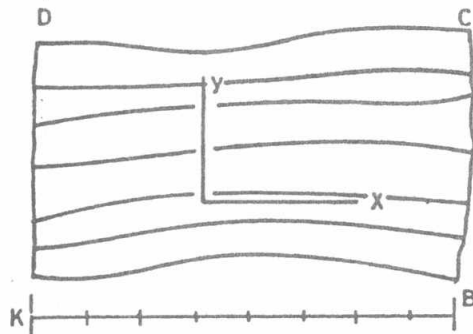


Fig. 4.

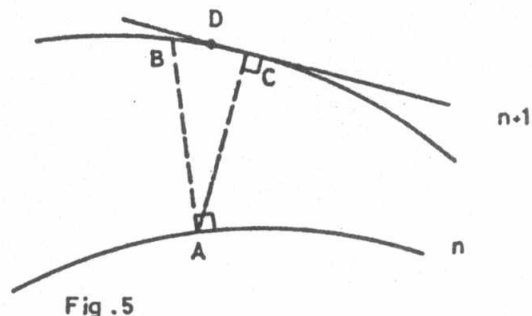


Fig. 5

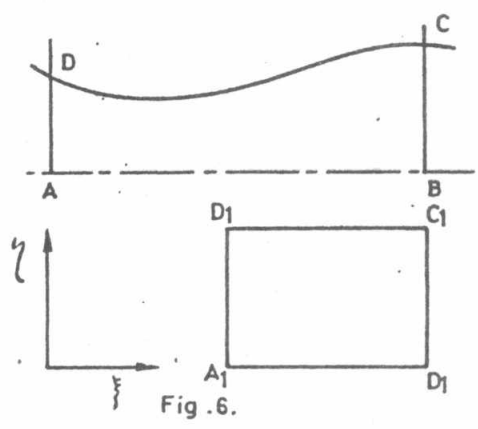
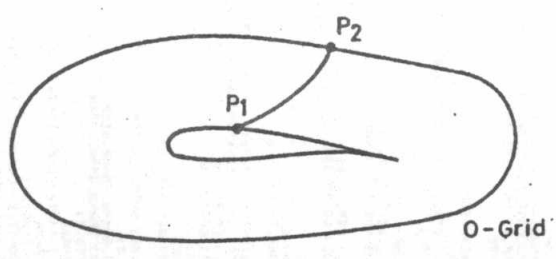
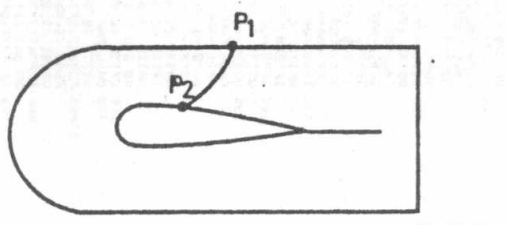
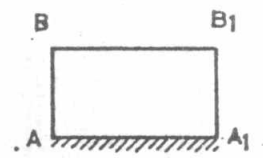


Fig. 6.



O-Grid



C-Grid

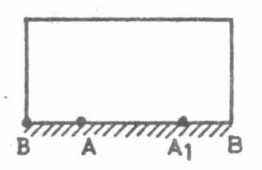
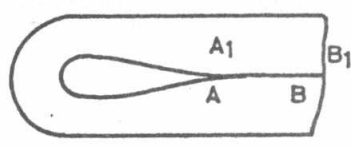


Fig. 7.

Fig. 8.

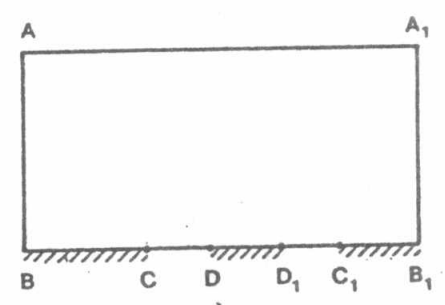
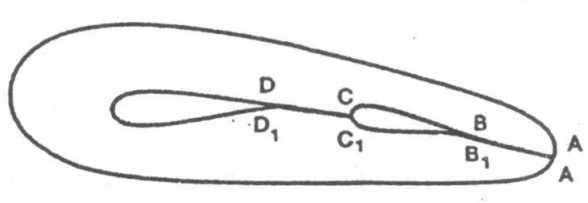


Fig. 9.

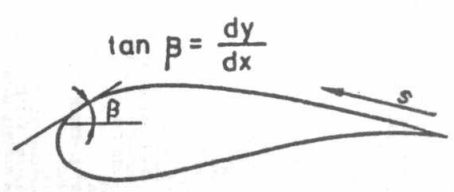


Fig. 10.









